Finite Element Model of Human Thermoregulation in Cold Conditions

BEE 4530 | Computer-Aided Engineering: Applications to Biological Processes

Aaron Berman, Yekaterina Khalatyan, Chris Umeki, Max Zhou
{ab986, yk598, ctu3, mz282}@cornell.edu

CONTENTS

I Executive Summary 4

II Introduction 5
- II-A Background . . . 5
- II-B Problem Statement . . . 5
- II-C Design Objectives . . . 6

III Schematic 6

IV Model implementation 9
- IV-A Governing Equation . . . 9
- IV-B Boundary conditions . . . 10
- IV-C Initial conditions . . . 11

V Mesh 11

VI Results and Discussion 13

VII Validation 16

VIII Sensitivity Analysis 19

IX Conclusion 20

Appendix 22
- A Blood flow . . . 22
- B Metabolism Term . . . 23
- C Solver configuration . . . 23
- D Data tables . . . 24

LIST OF FIGURES

1 Geometry schematic . . . 7
2 Geometry schematic . . . 8
3 Thermoregulation schematic . . . 9
4 Mesh cross-section . . . 11
5 Mesh quality . . . 12
6 Timestep convergence . . . 12
7 Mesh convergence . . . 13
8 Surface temperature sweep . . . 13
9 Temperature over time . . . 14
10 Ambient temperature . . . 15
11 Ambient thermoregulation . . . 16
12 Ambient temperature range at which shivering occurs . . . 17
13 Experimental skin temperature over time . . . 17
14 Simulated skin temperature over time . . . 18
15 Experimental shivering over time . . . 18

16 Thermoregulatory parameters over time 19
17 Sensitivity analysis 20
18 CPU Time 24

LIST OF TABLES

I Internal parameter data 24
II Geometry dimensions 25
III Distribution coefficients 25
IV External Parameters 25

I. Executive Summary

The human body can only function properly within a narrow range of temperatures. Therefore, the regulation of body temperature is a critical part of survival. Thermal homeostasis is maintained through complex feedback loops, with the body reacting to local temperature changes. The critical components of this feedback loop are linked to the skin temperature and the hypothalamus temperature. the skin is responsible for heat sensing, while the hypothalamus is the body's temperature control center.

In this study the effect of thermoregulation on the temperature of multiple domains throughout the body was considered, and an attempt to create a 3-dimensional model that accurately displays its effect on body temperature was attempted. To investigate the effect that thermoregulation has on maintaining temperature and to investigate the accurate temperature profile of the human body, COMSOL, a finite element software capable of running physics simulations, was utilized. There had been previous research on the topic that used only a few hundred nodes or used lumped parameters to simulate thermal regulation. Our model's geometry was 3-dimensional and inspired by the dimensions used in a previous model by Dr. Dusan Fiala [1].

To implement thermoregulatory effects, empirical formulas were found in previous literature for shivering, vasodilation and vasoconstriction among others. All empirical formulas were temperature sensitive and were functions of the skin temperature and/or the hypothalamus temperature. These effectors change the local heat generation terms and the local blood perfusion terms, both crucial components of the heat equation in biological systems. An initial simulation of the body temperature was run at cool environment with some air flow. The results showed a sharp decline in average skin and fat temperatures initially due to their proximity to the surface, while the average brain temperatures declined gradually and then flattened off within the first two hours. Simulations excluding different components of thermoregulation were also ran to portray the importance of thermoregulation in the body. The simulations without thermoregulatory components resulted in much lower brain temperatures, as expected . Furthermore, the magnitude of different effectors were measured, allowing for analysis on the importance of different ways body's thermoregulate. To validate the model, experimental data was compared to our simulated result. Experimental data regarding skin temperature over time, and shivering magnitude over time matched the overall trend of our data. Similarly, research on what external temperatures induce shivering were in line with the simulated results.

This model provides insight into the distribution of temperature across the human body and will provide the basis of a comprehensive human model applicable to a range of topics, such as clothing insulation and frostbite analysis. By incorporating empirical equations that are functions of temperature and having a 3D model that is heavily discretized, the model can accurately portray the body's temperature profile in cold climates.
Keywords: thermoregulation, weather, body heat, hypothermia, homeostasis

II. Introduction

A. Background

Thermoregulation is a key component of homeostasis, the state of steady internal conditions essential for life. Humans maintain this critical internal balance through a complex feedback loop between the hypothalamus and the body's blood vessels. The hypothalamus uses its own temperature and the skin temperature as determining factors in constricting or dilating blood vessels, which regulate local temperature. The hypothalamus and skin temperature also affect the shivering of the muscular regions of our body, which produce localized heat. This complex feedback loop, which reacts to ever changing internal temperature fluctuations, is essential to human life, but an accurate three-dimensional model is still lacking.

The first significant attempt at a computer model of human thermoregulation came almost 50 years ago, in 1971 [2]. This was a model designed for NASA by J.A.J. Stolwijk. Stolwijk used 25 different points in the body, which he called "nodes", and modeled the heat transfer with a "lumped-parameter" method, which sufficiently simplified the model to be run on the computing power available during that time. There has been more research into heat transfer and thermoregulation in humans, but the focus has been on a single body part [3], [4] or to discretize the problem into a few hundred nodes divided among body segments [1], [5], [6], many building off of Stolwijk's original model.

Segmented models assume that the temperature and physical parameters are uniform throughout the segment, which becomes invalid if there is localized heating and cooling between nodes. Likewise, models of a single body segment fail to take into account the global effect of blood circulation, which couples heating and cooling from distant body parts. In addition, some of the inputs to the thermoregulatory signal are from surface receptors on the head and skin, which provide further long-distance feedback effects. Our model builds off the Fiala model, which is heavily used as a starting point for other thermoregulation studies [6], [7]. Instead of using the 167 nodes in the original Fiala model, COMSOL was used to generate a finite element mesh, but using the same thermal and physical parameters as in the original model. Our model aims to validate and build upon the results of Fiala's nodal models, by relying on the integration of mesh domains rather than the summation of nodes.

Creating a more accurate computer model of human thermoregulation is worth pursuing, as it can be used to investigate temperature effects in various scenarios without the need for experimentation in uncomfortable or impossible conditions. For example, a thermoregulation model could be used to test space-suits without any need for experimentation in outer space. Optimized clothing, blankets, and so on could be designed using the computer thermoregulation model. Another possible application of this model is anesthesia, which can reduce cold response thresholds as well as the maximal response intensity [8].

B. Problem Statement

The objective of this research is to provide an accurate 3D model of human body temperature, when exposed to the elements, over time. Our model will incorporate convective cooling from the wind, radiative heat transfer from the Sun, conductive heat transfer occurring within body layers and heat transfer due to blood flow. To achieve meaningful results our model will also

include thermoregulatory effects, such as shivering, vasoconstriction, and vasodilation, to mimic the body's response to different temperatures. By performing ablation studies on various parts of the thermoregulatory system, we will examine the relative contribution of each part of the system. We also plan to perform sensitivity analysis on the effect of material properties on our results, because not all humans will have uniform material properties. This accurate 3D model of human body temperature can be utilized across many industries and provide essential insight into the effects of environmental conditions on temperature and the impact of clothing on temperature. Our model provides the foundational basis for these future tests, with an accurate, tested and validated human model that can be easily applied to other subjects.

C. Design Objectives

This study will contribute to the field of research on thermoregulation in the following ways:

1) Understanding the change of temperature over time when the body is exposed to varying external conditions.
2) Exploring the impact of thermoregulation on internal body temperature.
3) Determining the impact of different variables on internal temperatures by implementing a sensitivity analysis.

III. SCHEMATIC

This 3D model was created to mimic the geometry used by Dusan Fiala. Simplified model of the geometry of the body contains the following domains, from the top down: head, neck, torso (upper region is defined as the thorax, and the lower region is defined as the abdomen), and legs. Each of these have certain tissue layers arranged concentrically within. From outermost to innermost in each, these are as follows.

- head: skin, fat, bone, brain, hypothalamus
- neck: skin, fat, muscle, bone
- thorax: skin, fat, muscle, bone, lung
- abdomen: skin, fat, muscle, bone, viscera
- legs: skin, fat, muscle, bone

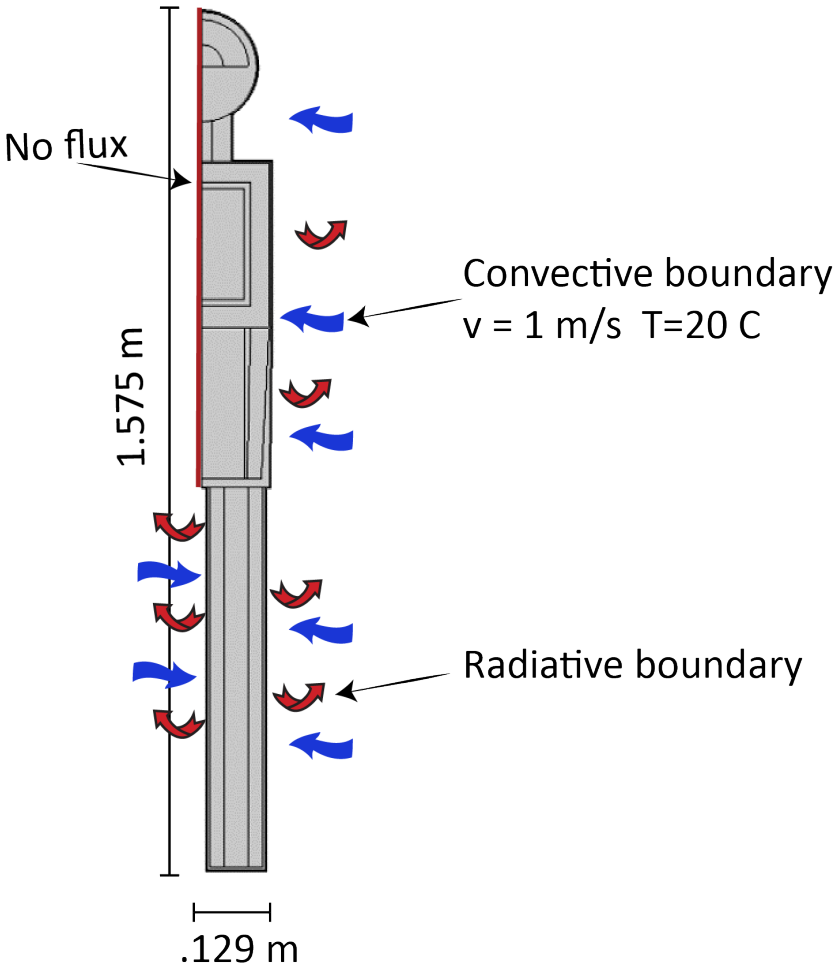

Fig. 1. A 2D schematic of the model. A quarter of the model is used due to two planes of symmetry. There is no heat flux at all planes of symmetry and a convective and radiative boundary along all of the skin.

The domains were selected based on their involvement in thermoregulation. For example the brain contains the hypothalamus. As shown earlier both the vasodilation term (16) and shivering heat (21) depend on the hypothalamus temperature $T_h y$. The legs were included in order to involve countercurrent heat exchange, because the countercurrent heat exchange coefficient h_x, used in (14), is zero outside the arms and legs. However, arms were not included because of the difficulty to implement the geometry in COMSOL. Taking advantage of two planes of symmetry, the geometry was simplified by cutting it into a quarter of the size. This allowed for the reduction of computational time, while including no new radical assumptions into the model. Unfortunately, this also means the model does not have a specific face component.

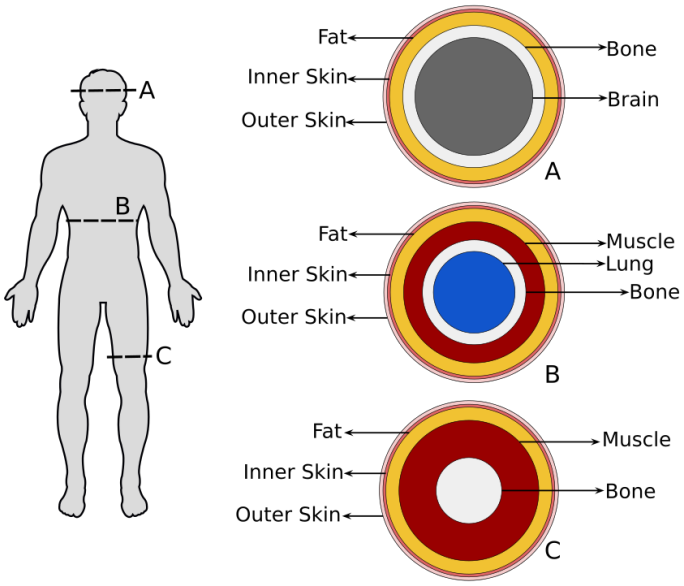

Fig. 2. Cut planes (left) and corresponding cross sections (right). A) Head B) Thorax C) Leg.

As shown in Figure 2 each domain is composed of multiple regions. The outer layer and second-most outer layer are always the skin and fat respectively. Every domain also included a bone region. Unique regions of note are the brain, the lung and the viscera. The brain is located in the head domain and contains the hypothalamus as a subregion. The hypothalamus is essential in this model and in real life for maintaining thermal homeostasis. The lung is locate in the torso and causes respiratory heat loss. The viscera is located in the abdomen and its high basal metabolic heat generation keeps the core warm.

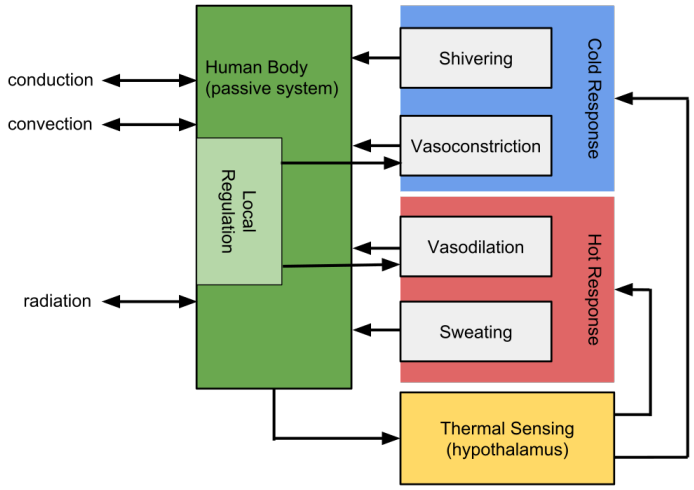

Fig. 3. Thermoregulatory processes. The left hand side displays the boundary conditions of the model. On the right the feedback loop between the hypothalamus and thermoregulatory effectors are displayed.

Figure 3 diagrams the feedback loop of the model. Thermal sensing by the hypothalamus and local regulation by the skin and muscle layers causes the feedback loop between the hot and cold response. These responses effect the body temperature which is the cause of the thermal regulatory feedback loop.

IV. Model Implementation

A. Governing Equation

The objective of the model is to find the temperature at each point in the domain over time. The function describing temperature (T) is $T(x, y, z, t)$ where x, y, z are spatial variables in the Cartesian plane and t is time.

Considering heat conduction, the rate $\dot{T}$ at which the material at a point will heat up or cool down is proportional to how much hotter or cooler the surrounding material is. This may be described by the Laplacian ∇^2 of the temperature T. The rate of the temperature change is proportional to Laplacian to the temperature by proportionality constant α.

$$\left(\frac{\partial T}{\partial t}\right)_{\text{conduction}} = \alpha \nabla^2 T \tag{1}$$

The coefficient α in the equation is related to the thermal conductivity k, the specific heat c, and the density ρ of the material. The thermal conductivity, specific heat and the density varies by domain.

$$\alpha = \frac{k}{\rho c} \tag{2}$$

$$\left(\frac{\partial T}{\partial t}\right)_{\text{conduction}} = \frac{k}{\rho c} \nabla^2 T \tag{3}$$

In the human body, metabolic heat generation adds to the rate of temperature change and will be assigned the variable (q_{m}). The value of this variable varies across different domains.

$$\rho c \left(\frac{\partial T}{\partial t} \right)_{\text{metabolic}} = q_{\text{m}} \tag{4}$$

Blood flow contributes to temperature change as well. Its effect may be described by Pennes bioheat equation shown below

$$\rho c \left(\frac{\partial T}{\partial t} \right)_{\text{blood flow}} = \rho_{\text{BL}} w_{\text{BL}} c_{\text{BL}} \left(T_{\text{BLa}} - T \right) \tag{5}$$

Where

ρ_{BL} is blood density
c_{BL} is blood specific heat
w_{BL} is blood perfusion rate, which varies by domain.

T_{BLa} is the arterial blood temperature within the body, which is governed by (14) derived below. Considering the contributions of convection, metabolic heat generation, and blood flow, the terms of (3), (4), and (5) are combined, producing our governing heat equation:

$$\rho c \left(\frac{\partial T}{\partial t} \right) = k \nabla^2 T + q_{\text{m}} + \rho_{\text{BL}} w_{\text{BL}} c_{\text{BL}} \left(T_{\text{BLa}} - T \right) \tag{6}$$

There are several calculated variables that effect q_{m} and w_{BL}. q_{m} is composed of basal metabolic heat generation, the change in metabolic heat generation, heat generation of shivering and exercise and the heat loss due to respiratory cooling. The change in metabolic heat generation is an Arrhenius equation, so that it decreases as the local temperature decreases. Shivering is a function of both the temperature change in the hypothalamus and the temperature change of the corresponding skin region. The empirical equation for shivering is in watts, so its value is divided by the muscle volume and then weighted by an empirical constant to be in $\frac{W}{m^3}$. There is no exercise occurring in the model so that term is ignored. The heat loss due to respiration is a function of the total metabolic heat in the body, the local temperature and the ambient temperature. This loss only occurs in the neck muscle and the lungs. Refer to subsection B for the equations for metabolism terms and thermoregulatory control terms.
w_{BL} is composed of an initial perfusion rate and a natural change in perfusion due to the local basal metabolism. Due to the local basal metabolism being a positive function of temperature, as temperature decreases so to does blood perfusion. w_{BL} of the skin regions are also reliant on an empirical formula that is reliant on the vasoconstriction and vasodilation. Each is a function of both the temperature change in the hypothalamus and the temperature change of the corresponding skin region. Refer to subsection A for the equations for blood flow, and thermoregulatory control terms.

B. Boundary conditions

Radiative heat transfer (7) occurs on all exposed surfaces of the skin where σ is the Stefan-Boltzmann constant, $\epsilon_{\text{env}} = 1.0$ and $\epsilon_{\text{bs}} = 0.95$ are the surface emissivity of the radiant envelope and body sector, respectively, $\phi_{\text{bs-env}}$ is a view factor, T_{bs} is the surface temperature of the body sector, and T_{env} is the surface temperature of the radiant envelope.

$$q_{\text{rlw}} = \sigma \epsilon_{\text{bs}} \epsilon_{\text{env}} \phi_{\text{bs-env}} \left[T_{\text{bs}}^4 - T_{\text{env}}^4 \right] \tag{7}$$

A convective heat boundary condition also is applied at the skin. The geometry of the model is roughly that of a cylinder. Therefore, the convective boundary condition was implemented utilizing COMSOL's convective correlation heat flux function. This function allows for a nonlinear boundary condition, at the cost of approximating the models overall geometry. A radius of the approximated cylinder and the ambient air velocity were inputted to create this boundary condition.

C. Initial conditions

The initial temperature was set to $34.4\,^{\circ}\mathrm{C}$ at the skin and $37\,^{\circ}\mathrm{C}$ within all other domains.

V. MESH

The implemented mesh of this model is varied by domain (Figure 4). The skin and fat domains of the model were given the finest meshing due to their proximity to the external environment, where the largest temperature gradient occurs. Domains that are further away from the skin surface, or had intermediate thicknesses, were given a coarser mesh. The largest domains and those that are furthest from the skin were given the coarsest meshing. These regions are the least susceptible to large temperature gradients, allowing a coarse mesh to calculate similar temperatures to that of a finer mesh while decreasing the computation time.

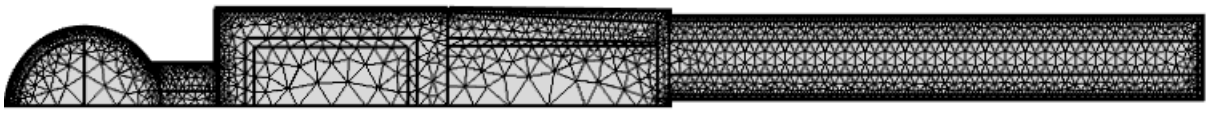

Fig. 4. Mesh cross-section. The meshing is much finer at the skin and fat and becomes progressively coarser the further the region is from the skin.

There were concerns that the varied meshing would contribute to a lower mesh quality throughout the model. Figure 5 is a mesh quality graph of the neck domain. This domain was chosen due to various intersections of fine mesh regions which could contribute to low mesh quality. However, as shown in Figure 5 the overall mesh quality is fairly high except for the neck skin and fat layers, which are incredibly thin and a low quality mesh was needed to be used to properly mesh it.

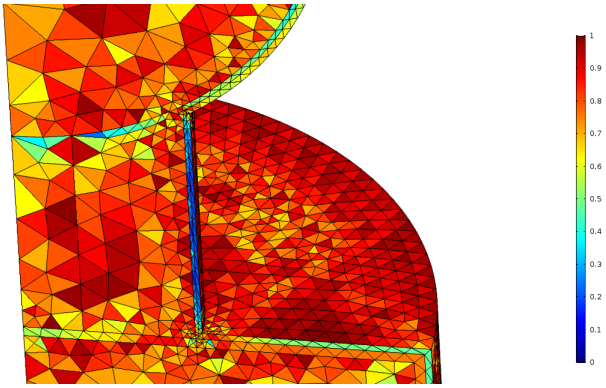

Fig. 5. Mesh quality is displayed. A value closer to 1 indicates a higher quality mesh which is better for calculations. Low quality mesh can lead to discretization error. The domain displayed is the neck, intersecting the head and the thorax.

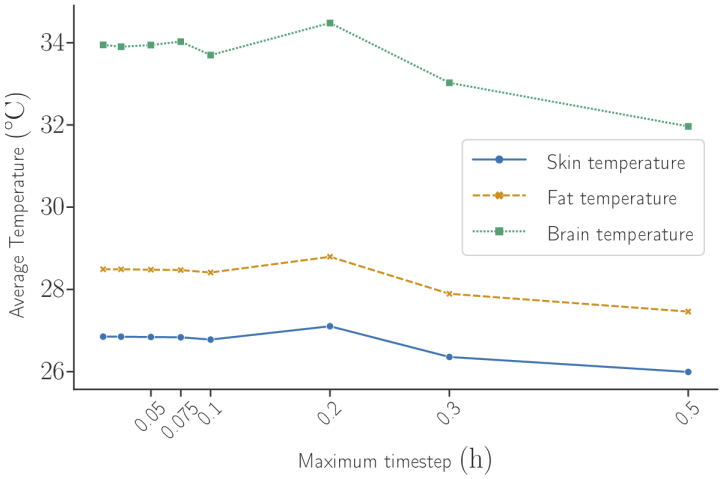

Fig. 6. Timestep convergence. The simulation was run over 5 hours with differing maximum time steps. The final average skin, fat and brain temperature were recorded and plotted.

A timestep convergence test was run by simulating the model at differing maximum time steps. The results are displayed in Figure 6. As the maximum timestep dipped below about $1\,\mathrm{h}$, the dependent variable, the average brain temperature, flattened off and converged. Further simulation of the model was done using a maximum timestep of $0.075\,\mathrm{h}$.

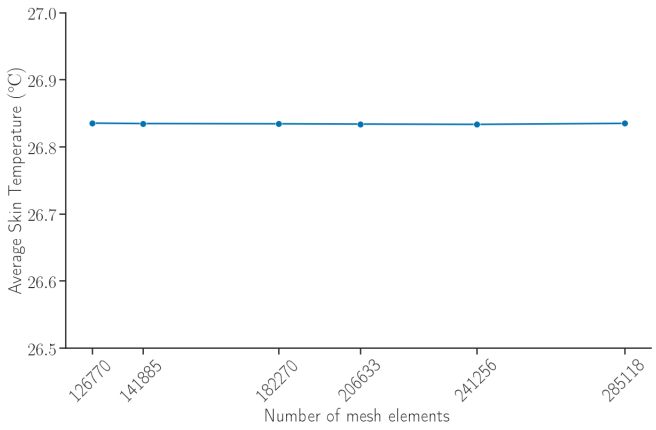

Fig. 7. Mesh convergence. The simulation was run over 5 hours with differing number of mesh elements. Only the final average skin temperature is plotted.

A mesh convergence test was run over varying coarseness of mesh with a maximum timestep of $0.075\,\mathrm{h}$. The mesh convergence, shown on Figure 7, displays negligible changes on the order of $0.001\,^{\circ}\mathrm{C}$ in temperature with varied quantity of mesh elements. Only the final average skin temperature is recorded because the skin is the most likely region to have discretization error due to the large temperature gradient at the surface. It was determined that the mesh had converged and the model utilized a mesh that contained 182,270 mesh elements.

VI. Results and Discussion

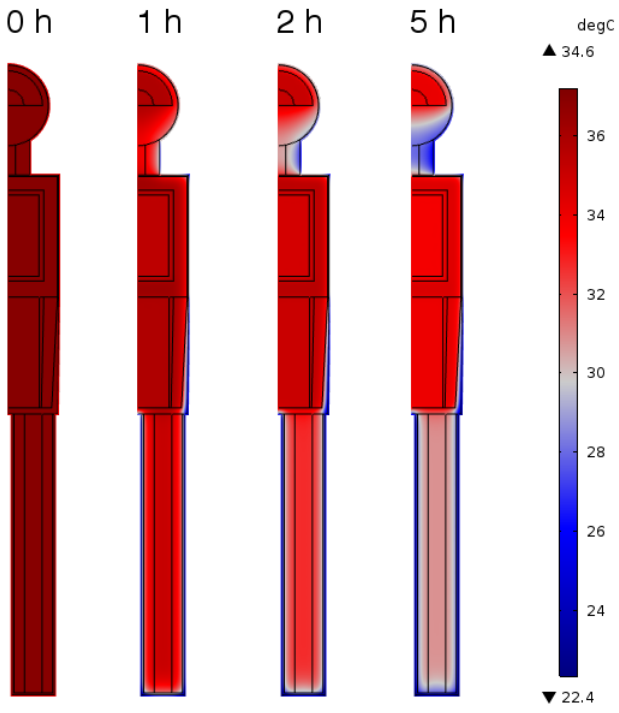

Fig. 8. Surface temperature of a cut plane through the coronal plane of symmetry. The simulated ambient temperature is $20\,^{\circ}\mathrm{C}$ and the air velocity is $1\,\mathrm{m\,s^{-1}}$. The model was ran over a 5 hour simulated period.

Figure 8, a surface plot of the simulated temperature, shows how there is the sharpest temperature decrease in the neck and legs. This is because the countercurrent heat exchange in the legs causes the outgoing blood flow to the legs to lose heat more quickly. Due to respiratory cooling and low basal metabolic heat generation the neck cools quickly. The core and brain maintain relatively warmer temperatures due to the high basal metabolic heat generation of these regions, along with the implementation of thermoregulation, which prioritizes the warmth of the brain over the rest of the body.

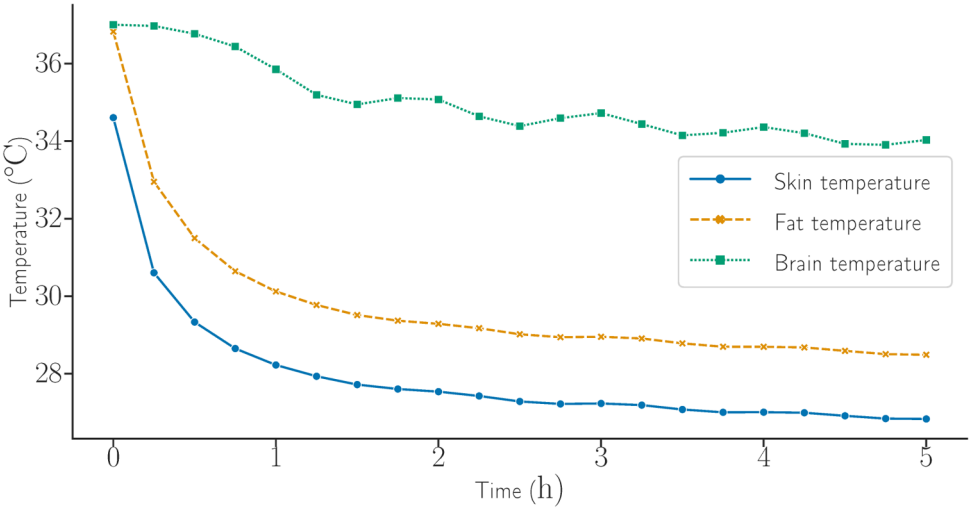

Fig. 9. Temperature over time of the designed model at different domains. Conditions are an ambient temperature of 20°C, and air velocity of $1\,\mathrm{m\,s^{-1}}$. The skin temperature is a weighted volumetric average over the whole domain, fat and brain temperature are unweighted volumetric averages of their respective domains.

As displayed in Figure 9, at early times the skin and fat temperature drop drastically due to the large temperature gradient at the surface, and their proximity to the surface. By the two hour mark, both the average fat and skin temperature flatten off as the body has reached thermal equilibrium. In contrast, the brain temperature decreases gradually over the first two hours, and by the second hour has reached a consistent oscillatory state. This gradual decline and later oscillation can be explained by the thermoregulation of the body. The brain's distance from the skin surface, but also the effects of vasoconstriction, basal heating and shivering keep the decline gradual. The oscillating temperatures can be explained by the body overcompensating when heating the body, therefore causing the hypothalamus temperature to hover around this apparent threshold value of about 34°C.

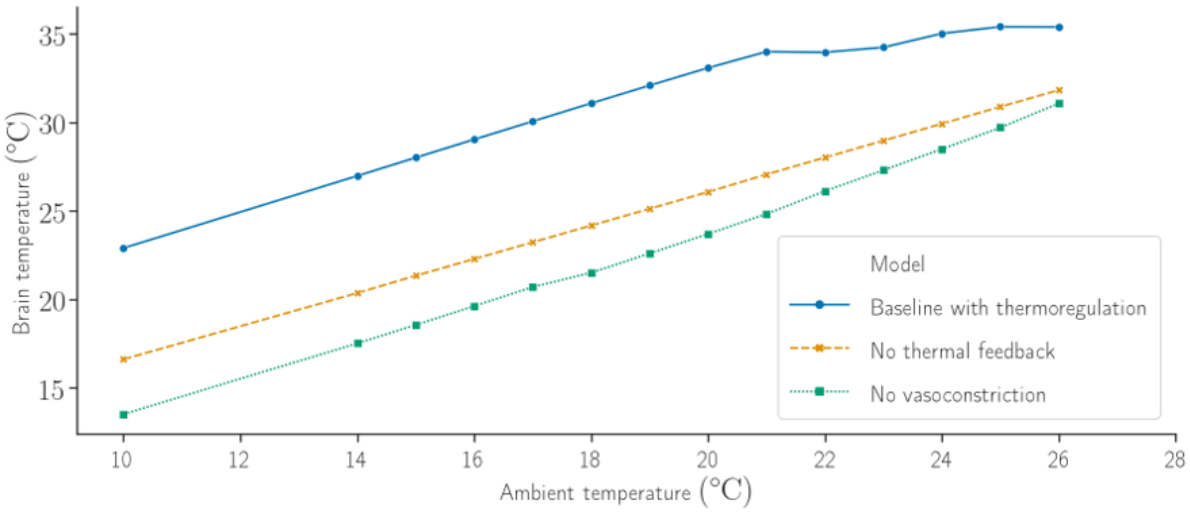

Fig. 10. Brain temperature over differing ambient temperatures . The ambient air velocity was maintained at $1\,\mathrm{m\,s^{-1}}$ and results are collected at the $5\,\mathrm{h}$ mark. The baseline with thermoregulation is plotted alongside two variants. One variant excludes all thermoregulatory effects that are temperature dependent. The other variant excludes vasoconstriction.

To explore the effects thermoregulation had on the brain two variants were ran on the original model and compared them to our original model (Figure 10). The effect on the brain was explored due to its out-sized role in survival and its important role in thermoregulation. One variant excluded all terms that were temperature dependent. This includes the exclusion of shivering, vasoconstriction, vasodilation and the change in basal metabolic heating that occurs due to temperature changes. The other variant on the model excluded only local and global vasoconstriction from the model. Both variations resulted in lower brain temperatures across a sweep of differing ambient temperatures. This was as expected because thermoregulation is the main mechanism that controls the brain temperature. A surprising, yet easily explainable result, was that the no thermal feedback variant experienced higher temperatures than the vasoconstriction variant. The no thermal feedback variant did not include the reduction in metabolic heat generation that occurs due decreasing temperature. This mechanism acts as a positive feedback loop that was excluded in this variant, but was included in the vasoconstriction variant. Importantly, this effect decreases as ambient temperature increases due to the decreasing effect of vasoconstriction on the model. Under these conditions, the simulated human can maintain thermoneutrality until about $21\,^{\circ}\mathrm{C}$, as seen by the brain temperature staying level with respect to ambient temperature.

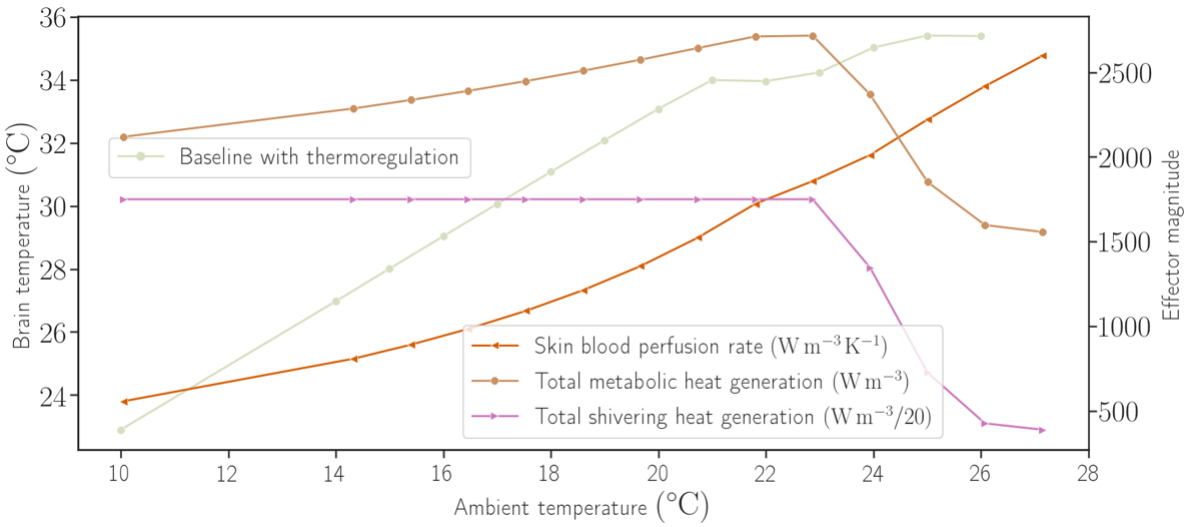

Fig. 11. Brain temperature and effector magnitude at differing ambient temperatures. The ambient air velocity was maintained at $1\,\mathrm{m\,s^{-1}}$ and results are collected at the $5\,\mathrm{h}$ mark.The magnitude of skin blood perfusion, shivering and total metabolic heat generation are displayed.

To examine how the magnitude of different effectors changed over differing ambient temperatures, a temperature sweep similar was utilized (Figure 11). As ambient temperature increased the blood perfusion rate of the skin also increased. This is expected because at warmer temperatures vasoconstriction will decrease and vasodilation will increase resulting in greater blood flow. From 10°C to 23°C the magnitude of shivering was constant, however at 24°C a sharp decline in the magnitude of shivering occurred. It is presumed that by 26°C the body has reached thermal neutrality and no longer needs thermoregulatory cooling to maintain internal temperatures. This sharp decline in metabolic heat generation corresponds to that of shivering's decline. Total heat generation increases as the external temperature increases until 22 °C, and then sharply declines. This occurs due to the change in basal metabolic heat generation decreasing as temperature increases, while shivering remains at the theoretical limit for a human. Once shivering's magnitude declines, so does the total metabolic heat generation. This indicates that shivering is a major component of the total heat generation in the body.

VII. Validation

To validate the model, multiple experiments were utilized to compare the experimental data to the simulated results. This data was utilized to validate both the magnitude of the thermoregulatory effectors and the overall change in body temperature over time.

In a 2014 study by Kingma et al.[9], a biophysical model of heat transport in the body was created to analyze when thermoregulation effectors like sweat and shivering would begin to occur. As seen in Figure 11, shivering, in the model, ends at an ambient temperature of 26 °C. — which corresponds with the end of the classical thermoneutral zone described in the paper, 25.9 °C , for a nude body considering only basal metabolism. This comparison shows that the shivering effector is active within a realistic and expected temperature range (Figure 12).

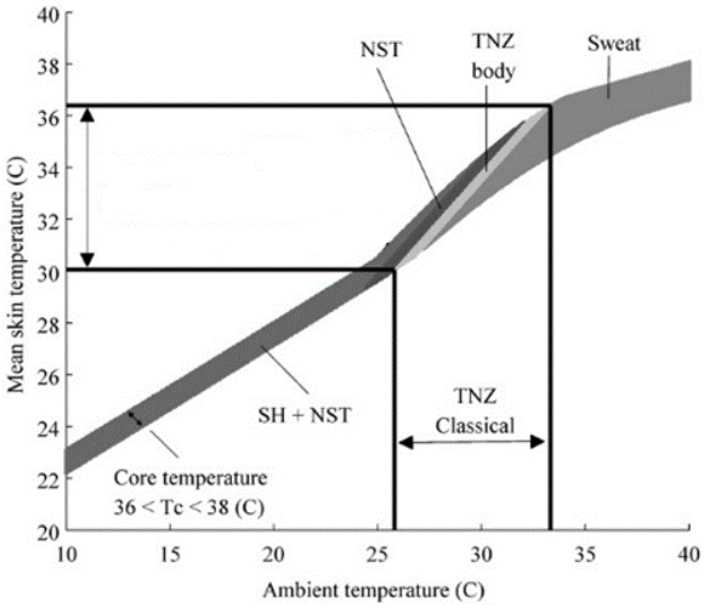

Fig. 12. Ambient temperature range at which shivering occurs [9]. The band that begins on the left hand size represents shivering. Shivering occurs up to 26°C, and then dissipates quickly.

In addition, two in vivo studies were used to validate the model. In one experiment [10], men were exposed to an air temperature of 17 °C for 60 minutes, wearing only swimming trunks. Men were in two groups: young (20–25 years) and older (60–71 years), matched for body fatness and surface area/mass ratio. Figure 13 displays the results, with older men represented in white and younger men in black. Figure 14, our model's results for a 20 °C ambient temperature follow a very similar trend, with skin temperature drastically cooling at earlier times and then slowly leveling off to about the same temperature as it does in the experiment (approx. 29 °C), after 60 minutes. The similar cooling in our model as opposed to the experimental data at a somewhat lower temperature (17 vs 20 °C) may be at least partially explained by the wearing of swimming trunks, which would conserve heat, and geometry differences from our simplified model to real humans.

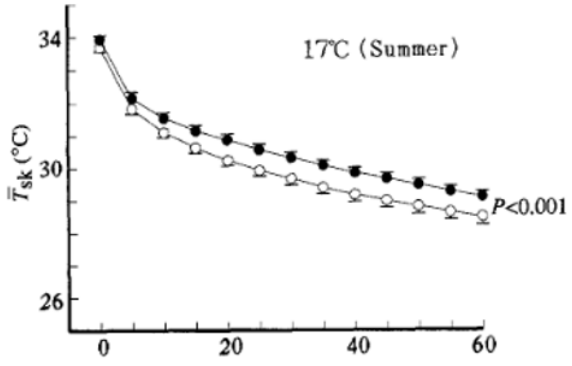

Fig. 13. Experimental skin temperature over time at 17°C [10]. The white dots are results from older men, while black dots are results from younger men. A sharp decline in skin temperature occurs for both.

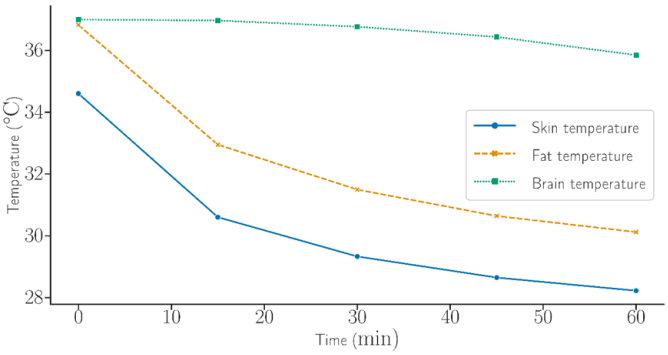

Fig. 14. Simulated skin temperature over time at 20°C. A sharp decline in skin temperature occurs.

In a third experiment [11], seven men underwent 1-hour of daily cold-water immersion (14 °C) for 7-consecutive days. Before the immersions, they were tested at pre-acclimation, with an immersion of 150 minutes, altering the water temperature to keep the skin at 26 °C. After the 7-day acclimation, the same experiment was repeated. Shivering intensity over time, measured in percent of a maximum voluntary muscle contraction, is shown below in Figure 15. White circles are pre-acclimation and black circles represent post-acclimation results. Alongside is a plot of total shivering heat generation over time in our computer model, while the ambient temperature is kept at 20 °C. The long-term trend of shivering rising to some value and then leveling off in the experiment is consistent with the model. However, over the short term the model's results are more in line with the post-acclimation results. This might be explained by empirical formulas being derived from subjects who were already acclimated to cold temperatures, however this is only speculation.

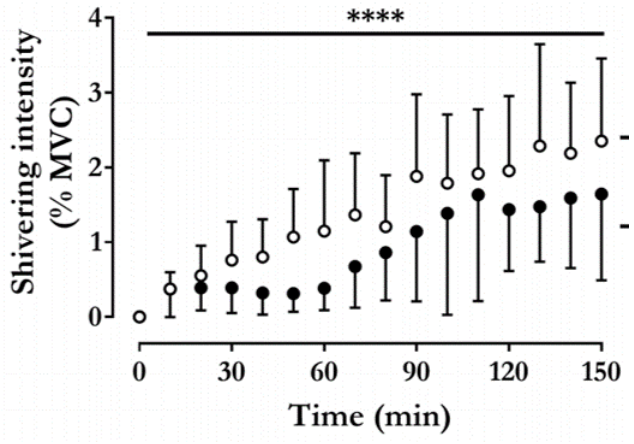

Fig. 15. Experimental value of shivering intensity rises and levels off with time. The white dots are results pre-acclimation to cold weather. Black dots are results post-acclimation to cold weather [11].

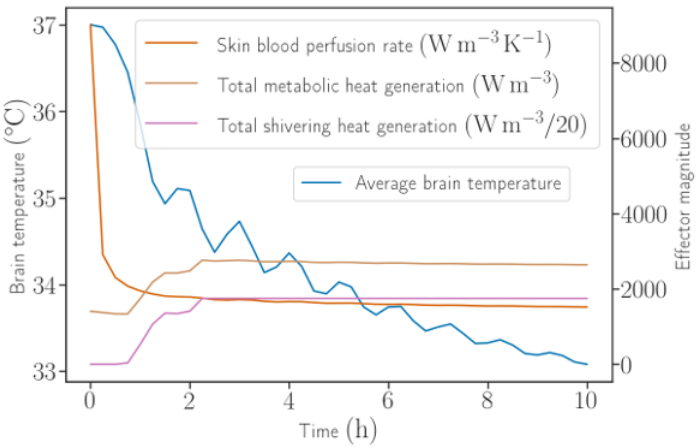

Fig. 16. Cold response in our model. Shivering heat generation and total metabolic heat generation rise and leveling over time. Skin blood perfusion drop due to vasoconstriction.

VIII. Sensitivity Analysis

As seen in Figure 17, the brain temperature is sensitive to some changes in parameter value. A change of about $0.4\,^{\circ}\mathrm{C}$ is determined to be significant, due to how narrow the functional brain temperature range is. The parameters tested for sensitivity are thermal conductivity, heat capacity, basal metabolic heat generation, blood flow, shivering and the change in basal metabolic heat generation across the entire body. The first two parameters were selected due to being material properties that vary between individuals. Basal metabolic heat generation ($q_{\mathrm{m,bas}}$) was selected also due to the likely variation between individuals. The last three parameters were selected to see how sensitive the model was to parameters that effect or are effected by the body's thermoregulation.

The parameter change that resulted in the biggest difference between actual simulation and sensitivity analysis result was that of shivering. This indicates that shivering has a profound effect on the body temperature. These results also indicate that the model was sensitive to the value of thermal conductivity (k). This is likely due to the importance of the fat layer as an insulator and by changing the insulation of the body the internal temperature of the body changes fairly significantly. Another significant parameter was the basal metabolic heat generation ($q_{\mathrm{m,bas}}$), which is unsurprising due to the significant amount of heat the body generates. These results are significant because they indicate that changes to the parameters, many of them that in reality are unique to each individual, can have some significant changes. This needs to be taken into account when applying this model to individuals, due to the variation across people.

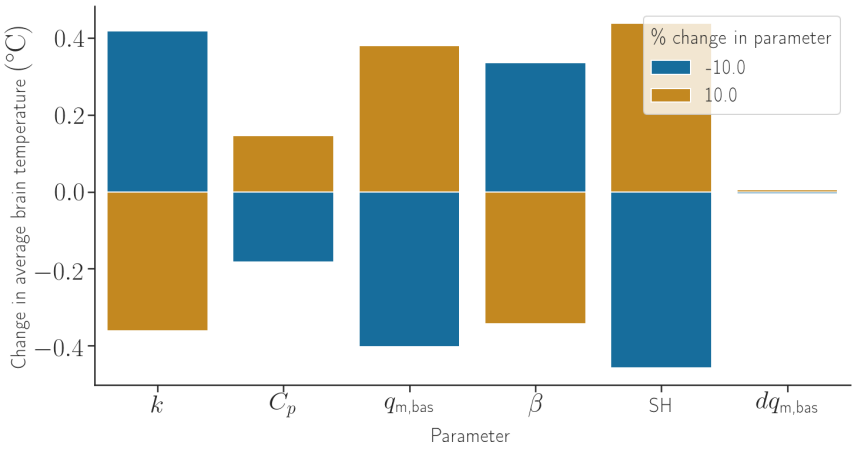

Fig. 17. Sensitivity analysis of average brain temperature with respect to thermal conductivity, heat capacity, basal metabolic heat generation, blood flow, shivering and the change in basal metabolic heat generation. All parameters were run at values 10% higher and lower than their actual values, and were applied across the entire body. The data was collected at the 5 hour mark, with ambient temperature of $20\,^{\circ}\mathrm{C}$ and air velocity of $1\,\mathrm{m\,s^{-1}}$.

IX. Conclusion

The model completed its design objectives by providing insight in the way the internal body temperature changes over time and under different external conditions. The fat and skin regions consistently underwent sharp drops in temperature, while the brain underwent a gradual and stabilizing decline. The body should prioritize the warmth of the brain over its externalities and the results in this paper are in line with the expected results and some experimental results. Furthermore, the model explored and explained the impact thermoregulation has on the internal body temperature. Variants of the model without some thermoregulatory effects resulted in considerably lower temperatures, indicating the importance of considering thermoregulatory effects when modeling the human body. Lastly, the use of sensitivity analysis provided clarification on the crucial components of thermal regulation. All humans are different and a sensitivity analysis allows for the understanding of which parameters can be changed in humans, but still achieve fairly accurate results using this model.

For future work, the inclusion of sweating and evaporative cooling from the skin would be implemented. This would allow for he simulation of the body in warmer climates instead of only cold ones. The implementation of differing clothing layers would also be a good addition to this model. The use of this model is most likely in the fashion industry, so a better understanding of how the inclusion of insulation layers would effect the body temperature would be useful. This could easily be implemented through the addition of another layer that covers the torso and abdomen and simulates a shirt. A similar approach could be taken for the legs to simulate pants.

There are some limitations of this model. The first is the assumption of the geometry being used. The geometry is composed of simple intersecting geometric shapes, which does not fully capture the geometry of a human body. In fact, Fiala's original geometry doesn't even maintain continuity between different elements when actually modeled in 3D. Another limitation is the the implementation of the external conditions. Including fluid flow over the entire body could produce more realistic results than using the empirical relationship for forced convection over a cylinder. This model was also unable to handle the time-derivative part of the shivering formula due to the

enormous memory usage it entailed. This removed a damping effect on those effectors, resulting in erroneous oscillations of core temperature due to shivering's out of phase oscillations. Even with these limitations, this model provides a strong starting point for studying thermoregulation in a 3-dimensional model.

This model primarily addresses the economic constraints inherent in design contexts. When designing new clothing, for example, a detailed simulation allow a company to evaluate its insulating properties and rapidly iterate on the design without having to set up production lines to create costly physical prototypes and move on to human or mannequin testing.

APPENDIX

A. *Blood flow*

Defining arterial blood temperature T_{BLa}:

First, define $\beta_{0,\text{r}}$ as the time-dependent calorimetric equivalent of the nodal blood flow rate, such that

$$\beta_0, r = \rho_{\text{BL}} w_{\text{BL},r} c_{\text{BL}} \tag{8}$$

Blood flow is a function of metabolic heat generation in the body and changes such that

$$\Delta\beta_r = \mu_{\text{BL}} \Delta q_{\text{m}} \tag{9}$$

Total blood flow in the region is defined as β_r

$$\beta_r = \beta_{0,\text{r}} + \Delta\beta_r \tag{10}$$

Next, the variables C_r and Q_r are defined such that they are integrals over all the tissue layers in a domain r. A domain refers to a part of the body (trunk, head, leg, etc.) and a tissue layer may be fat, skin, muscle, bone, etc..

$$C_r = \int \beta_r dV \tag{11}$$

$$Q_r = \int T\beta_r dV \tag{12}$$

h_x is an overall countercurrent convective heat transfer coefficient, whose values are known. Based on Fiala paper (2012), T_{BLp}, the equilibrium blood pool temperature is

$$T_{\text{BLp}} = \frac{\sum_{i}^{tissue} \left(\frac{C_r}{h_{i,x}+C_r} \cdot Q_r \right)}{\sum_{i}^{\text{tissue}} \left[\frac{(C_r)^2}{h_{i,x}+C_r} \right]} \tag{13}$$

Note that if there is no countercurrent heat exchange ($h_x = 0$), then $T_{\text{BLa}} = T_{\text{BLp}}$. And according to the same paper,

$$T_{\text{BLa}} = \frac{T_{\text{BLp}} C_r + h_x Q_r / C_r}{h_x + C_r} \tag{14}$$

Define $\beta_0 = \rho_{\text{BL}} w_{\text{BL}} c_{\text{BL}}$ as a basal time-dependent calorimetric equivalent of the blood flow rate (units of $\text{Wm}^{-3}\text{K}^{-1}$). In the skin, this is modified by the local skin temperature and by vasoconstriction CS and dilation DL as follows:

$$\beta_i = \frac{\beta_{0,i} + \alpha_{dl,i} DL}{1 + \alpha_{cs,i} CS \exp(-DL/80)} \cdot 2^{\frac{T_{\text{sk}} - T_{\text{sk},0}}{10}} \tag{15}$$

$$DL = 21[\tanh(0.79\Delta T_{\text{sk,m}} - 0.70) + 1]\Delta T_{\text{sk,m}} + 32[\tanh(3.29\Delta T_{\text{hy}} - 1.46) + 1]\Delta T_{\text{hy}} \tag{16}$$

$$CS = 35[\tanh(0.34\Delta T_{\text{sk,m}} + 1.07) - 1]\Delta T_{\text{sk,m}} + 3.9\Delta T_{\text{sk,m}} \frac{dT^{(-)}_{\text{sk,m}}}{dt} \tag{17}$$

where $T_{\text{sk,m}}$ is the average skin temperature at that time, $T_{sk,0}$ is a reference skin temperature, $\alpha_{dl,i}$ and $\alpha_{cl,i}$ are distribution coefficients of relative constriction/dilation for the i-th element, and $\beta_{0,i}$ is the basal blood flow for skin element i. Hypothalamus temperature T_{hy} will be the average brain tissue temperature.

B. Metabolism Term

The terms in this section are empirically derived.

Metabolic heat generation (18) has a basal rate setpoint $q_{\text{m,bas,0}}$ from the literature [12] as well as additional response factors.

$$q_{\text{m}} = q_{\text{m,b,0}} + \Delta q_{\text{m}} \tag{18}$$

$$\Delta q_{\text{m}} = \Delta q_{\text{m,bas}} + q_{\text{m,sh}} + q_{\text{m,w}} \tag{19}$$

The additional factors are broken down in (19) to basal rate change $\Delta q_{\text{m,bas}}$, shivering heat $q_{\text{m,sh}}$, and exercise $q_{\text{m,w}}$.

$$\Delta q_{\text{m,bas}} = q_{\text{m,bas,0}} \left[2^{\frac{T-T_0}{10}} - 1 \right] \tag{20}$$

$$Q_{\text{m,sh}} = 10[\tanh(0.48\Delta T_{\text{sk,m}} + 3.62) - 1] - 27.9\Delta T_{\text{hy}} - 1.7\Delta T_{\text{sk,m}} \frac{dT_{\text{sk,m}}}{dt} - 28.6\text{W} \tag{21}$$

$$q_{\text{m,w}} = 0 \tag{22}$$

The empirically derived formulas for basal rate change (20) and shivering (21) were used, and exercise was set to zero (22) because the human model is stationary. Note that $Q_{\text{m,sh}}$ is a total shivering heat, so volumetric shivering heat is $q_{\text{m,sh}} = \frac{Q_{\text{m,sh}}}{V_{muscle}}$. All $q_{\text{m,sh}}$ was divided by four, due to the model only being one quarter of teh total geometry, while the shivering magnitude is written to be applied over the entire body The maximum shivering magnitude in watts, according to empirical data, is 350 W, so the magnitude in the model was capped at $350/4$ W.
Fiala's [12] values for material and other bodily properties were utilized.
Respiratory heat loss equation is defined by the summation of two different equations ((25)), both functions of the total basal metabolic heat generation and the ambient air temperature. First the enthalpy loss due to the air is defined as E_{rsp}, while the dry heat loss is defined as C_{rsp}

$$E_{\text{rsp}} = 3.233 * (0.0277 - 6.5 * 10^{-5} * T_{\text{a}} - 4.91 * 10^{-6} * p_{\text{a}}) * \int q_{\text{m}} dV \tag{23}$$

$$C_{\text{rsp}} = 1.44 * 10^{-3} * (32.6 - 0.934 * T_{\text{a}} + 1.96 * 10^{-4} * p_{\text{a}}) * \int q_{\text{m}} dV \tag{24}$$

$$Q_{\text{rsp}} = -(E_{\text{rsp}} + C_{\text{rsp}}) \tag{25}$$

T_{a} is the predefined ambient air temperature. p_{a}, is the water vapor pressure in the air. A humidity of zero was assumed so that p_{a} was 0.

C. Solver configuration

The solver used is the default iterative solver from COMSOL for time-dependent problems: Geometric Multigrid with GMRES as the solver. Two changes were made: first, the maximum timestep for the solver was set to be the `ts` variable (which was set to $0.075\,\text{h}$ in most cases). Second, the "Fully Coupled" node was modified so that the "Jacobian update" field was set to "On every iteration." This was done in order to help the solver converge on a solution. Tolerances were set to COMSOL's default (0.1 for absolute tolerance, 1 for tolerance factor, physics controlled relative tolerance). A screenshot of a portion of the log for a typical run is shown in Figure 18

```
Time-stepping completed.
Solution time: 2058 s. (34 minutes, 18 seconds)
Physical memory: 3.5 GB
Virtual memory: 3.9 GB
Ended at 29-Apr-2019 10:45:19.
----- Time-Dependent Solver 1 in Study 1/Solution 1 (sol1) ---------------------->
```

Fig. 18. Memory usage and runtime for a typical simulation.

D. Data tables

Most parameter data was directly from Fiala's model [1] for consistency.

TABLE I
INTERNAL PARAMETER DATA

Element	Material	Conductivity k ($\mathrm{W\,m^{-1}\,K^{-1}}$)	Density ρ ($\mathrm{kg\,m^{-3}}$)	Heat capacitance c ($\mathrm{J\,kg^{-1}\,K^{-1}}$)	Blood perfusion $w_{\mathrm{bl},0}$ ($\mathrm{L\,s^{-1}\,m^{-3}}$)	Basal metabolism $q_{\mathrm{m},0}$ ($\mathrm{W\,m^{-3}}$)
Head	Brain	0.49	1080	3850	10.1320	13400
	Bone	1.16	1500	1591	0.0000	0
	Fat	0.16	850	2300	0.0036	58
	Skin	0.47	1085	3680	5.4800	368
Neck	Bone	0.75	1357	1700	0.0000	0
	Muscle	0.42	1085	3786	0.5380	684
	Fat	0.16	850	2300	0.0036	58
	Skin	0.47	1085	3680	6.8000	368
Thorax	Lung	0.28	550	3718	Cardiac output	600
	Bone	0.75	1357	1700	0.0000	0
	Muscle	0.42	1085	3768	0.5380	684
	Fat	0.16	850	2300	0.0036	58
	Skin	0.47	1085	3680	1.5800	368
Abdomen	Viscera	0.53	1000	3697	4.3100	4100
	Bone	0.75	1357	1700	0.0000	0
	Muscle	0.42	1085	3768	0.5380	684
	Fat	0.16	850	2300	0.0036	58
	Skin	0.47	1085	3680	1.4400	368
Legs	Bone	0.75	1357	1700	0.0000	0
	Muscle	0.42	1085	3768	0.5380	684
	Fat	0.16	850	2300	0.0036	58
	Skin	0.47	1085	3680	1.0500	368

TABLE II
GEOMETRY DIMENSIONS

Element	Length (cm)	Material	Radius (cm)
Head	N/A	Brain	8.60
		Bone	10.05
		Fat	10.20
		Skin	10.40
Neck	8.42	Bone	0.75
		Muscle	0.42
		Fat	0.16
		Skin	0.47
Thorax	30.60	Lung	7.79
		Bone	8.91
		Muscle	12.34
		Fat	12.68
		Skin	12.90
Abdomen	55.20	Viscera	7.85
		Bone	8.34
		Muscle	10.90
		Fat	12.44
		Skin	12.60
Legs	139.00	Bone	2.20
		Muscle	4.80
		Fat	5.33
		Skin	5.53

TABLE III
DISTRIBUTION COEFFICIENTS

Element	Skin sensitivity a_{sk}	Dilation a_{dl}	Constriction a_{cs}	Shivering a_{sh}
Head	0.1432	0.0550	0.0040	0.0000
Neck	0.0715	0.0270	0.0140	0.0020
Thorax	0.2212	0.1410	0.0002	0.6305
Abdomen	0.2075	0.1610	0.0205	0.2400
Legs	0.3566	0.2290	0.3785	0.0813

The average skin temperature was weighted using the above skin sensitivity. The dilation, constriction and shivering coefficients were utilized to reduce the overall effect of each effector.

TABLE IV
EXTERNAL PARAMETERS

Parameter	Symbol	Value	Unit
Ambient temperature	T_{amb}	293.15	K
Ambient air velocity	v_{amb}	1.000	$\mathrm{m\,s^{-1}}$
Absolute pressure	P_{A}	1.000	atm
Surface emissivity	ε	0.950	1

The data in Table IV was used to establish the boundary conditions of convection and radiation.

REFERENCES

[1] D. Fiala, G. Havenith, P. Bröde, B. Kampmann, and G. Jendritzky, "UTCI-fiala multi-node model of human heat transfer and temperature regulation," *International Journal of Biometeorology*, vol. 56, no. 3, pp. 429–441, May 2012, ISSN: 0020-7128, 1432-1254. DOI: 10.1007/s00484-011-0424-7. [Online]. Available: http://link.springer.com/10.1007/s00484-011-0424-7 (visited on 02/15/2019).

[2] J. A. Stolwijk, "A mathematical model of physiological temperature regulation in man," 1971.

[3] D. B. Gurung, V. P. Saxena, and P. R. Adhikary, "FEM APPROACH TO ONE DIMENSIONAL UNSTEADY STATE TEMPERATURE DISTRIBUTION IN HUMAN DERMAL PARTS WITH QUADRATIC SHAPE FUNCTIONS," *Journal of applied mathematics & informatics*, vol. 27, no. 1, pp. 301–313, 2009, ISSN: 1598-5857. [Online]. Available: http://www.koreascience.or.kr/article/JAKO200906942471596.page (visited on 02/15/2019).

[4] M. A. Khanday, V. P. Saxena, A. H. Siddiqi, M. Brokate, and A. K. Gupta, "Finite element approach for the study of thermoregulation in human head exposed to cold environment," in *AIP Conference Proceedings*, Agra (India): AIP, 2009, pp. 375–385. DOI: 10.1063/1.3183555. [Online]. Available: http://aip.scitation.org/doi/abs/10.1063/1.3183555 (visited on 02/15/2019).

[5] S.-i. Tanabe, K. Kobayashi, J. Nakano, Y. Ozeki, and M. Konishi, "Evaluation of thermal comfort using combined multi-node thermoregulation (65mn) and radiation models and computational fluid dynamics (CFD)," *Energy and Buildings*, Special Issue on Thermal Comfort Standards, vol. 34, no. 6, pp. 637–646, Jul. 1, 2002, ISSN: 0378-7788. DOI: 10.1016/S0378-7788(02)00014-2. [Online]. Available: http://www.sciencedirect.com/science/article/pii/S0378778802000142 (visited on 02/15/2019).

[6] P. C. Cropper, T. Yang, M. Cook, D. Fiala, and R. Yousaf, "Coupling a model of human thermoregulation with computational fluid dynamics for predicting human–environment interaction," *Journal of Building Performance Simulation*, vol. 3, no. 3, pp. 233–243, Sep. 1, 2010, ISSN: 1940-1493. DOI: 10.1080/19401491003615669. [Online]. Available: https://doi.org/10.1080/19401491003615669 (visited on 02/15/2019).

[7] W. D. van Marken Lichtenbelt, A. J. H. Frijns, M. J. van Ooijen, D. Fiala, A. M. Kester, and A. A. van Steenhoven, "Validation of an individualised model of human thermoregulation for predicting responses to cold air," *International Journal of Biometeorology*, vol. 51, no. 3, pp. 169–179, Jan. 1, 2007, ISSN: 1432-1254. DOI: 10.1007/s00484-006-0060-9. [Online]. Available: https://doi.org/10.1007/s00484-006-0060-9 (visited on 02/15/2019).

[8] R. Lenhardt, "Chapter 37 - body temperature regulation and anesthesia," in *Thermoregulation: From Basic Neuroscience to Clinical Neurology, Part II*, ser. Handbook of Clinical Neurology, A. A. Romanovsky, Ed., vol. 157, Elsevier, 2018, pp. 635–644. DOI: https://doi.org/10.1016/B978-0-444-64074-1.00037-9. [Online]. Available: http://www.sciencedirect.com/science/article/pii/B9780444640741000379.

[9] B. R. Kingma, A. J. Frijns, L. Schellen, and W. D. V. M. Lichtenbelt, "Beyond the classic thermoneutral zone," *Temperature*, vol. 1, no. 2, pp. 142–149, 2014. DOI: 10.4161/temp.29702.

[10] Y. Inoue, M. Nakao, T. Araki, and H. Ueda, "Thermoregulatory responses of young and older men to cold exposure," *European Journal of Applied Physiology and Occupational Physiology*, vol. 65, no. 6, pp. 492–498, 1992. DOI: 10.1007/bf00602354.

[11] K. Gordon, D. P. Blondin, B. J. Friesen, H. C. Tingelstad, G. P. Kenny, and F. Haman, "Seven days of cold acclimation substantially reduces shivering intensity and increases non-shivering thermogenesis in adult humans.," *Journal of Applied Physiology*, 2019. DOI: 10.1152/japplphysiol.01133.2018.

[12] D. Fiala, K. J. Lomas, and M. Stohrer, "A computer model of human thermoregulation for a wide range of environmental conditions: The passive system," *Journal of applied physiology*, vol. 87, no. 5, pp. 1957–1972, 1999.